Adult Mouse Cortical Cell Taxonomy Revealed by Single-Cell Transcriptomics

Bosiljka Tasic, PhD

Allen Institute for Brain Science
Seattle, Washington

NOTES

Introduction

In the mammalian brain, the neocortex is essential for sensory, motor, and cognitive behaviors. Although different cortical areas have dedicated roles in information processing, they exhibit a similar layered structure, with each layer harboring distinct neuronal populations (Harris and Shepherd, 2015). In the adult cortex, many types of neurons have been identified by characterizing their molecular, morphological, connectional, physiological, and functional properties (Sugino et al., 2006; Rudy et al., 2011; DeFelipe et al., 2013; Greig et al., 2013; Sorensen et al., 2013). Despite much effort, however, objective classification on the basis of quantitative features has been challenging, and our understanding of the extent of cell-type diversity remains incomplete (Toledo-Rodriguez et al., 2004; DeFelipe et al., 2013; Greig et al., 2013).

Cell types can be preferentially associated with molecular markers that underlie their unique structural, physiological, and functional properties, and these markers have been used for cell classification. Transcriptomic profiling of small cell populations from fine dissections (Belgard et al., 2011; Hawrylycz et al., 2012) on the basis of cell surface (Cahoy et al., 2008; Zhang et al., 2010) or transgenic markers (Sugino et al., 2006; Doyle et al., 2008) has been informative; however, any population-level profiling obscures potential heterogeneity in collected cells. Recently, robust and scalable transcriptomic single-cell profiling has emerged as a powerful approach to characterization and classification of single cells, including neurons (Pollen et al., 2014; Usoskin et al., 2014; Macosko et al., 2015; Zeisel et al., 2015). We used single-cell RNA-sequencing (RNA-seq) to characterize and classify >1600 cells from the primary visual cortex in adult male mice. The annotated dataset and a single-cell gene expression visualization tool are freely accessible via the Allen Brain Atlas data portal (http://casestudies.brain-map.org/celltax).

Cell-Type Identification by Single-Cell Transcriptomics

To minimize the potential variability in cell types that results from differences in cortical region, age, and sex, we focused on a single cortical area in adult (8-week-old) male mice. We selected the primary visual cortex (VISp or V1), which receives and transforms visual sensory information and is one of the main models for understanding cortical computation and function (Glickfeld et al., 2014). To access both abundant and rare cell types in VISp, we selected a set of 24 transgenic mouse lines in which Cre, Dre, or Flp recombinases are expressed in specific subsets of cortical cells (Tasic et al., 2016). To isolate individual cells for transcriptional profiling, we sectioned fresh brains from adult transgenic male mice; microdissected the full cortical depth, combinations of sequential layers, or individual layers (L1, 2/3, 4, 5, and 6) of VISp; and generated single-cell suspensions using a previously published procedure (Sugino et al., 2006; Hempel et al., 2007) with some modifications (Fig. 1*a*) (Tasic et al., 2016). We developed a robust procedure for isolating individual adult live cells from the suspension by fluorescence-activated cell sorting (FACS); reverse-transcribed and amplified full-length poly(A)-RNA using the SMARTer protocol (SMARTer Ultra Low RNA Kit for Illumina Sequencing, Clontech, Mountain View, CA); converted the cDNA into sequencing libraries by tagmentation (Nextera XT, Illumina, San Diego, CA); and sequenced them using next-generation sequencing (NGS) (Fig. 1*a*). We established quality control (QC) criteria to monitor the experimental process and data quality (Tasic et al., 2016). Our final QC-qualified dataset contains 1679 cells, with >98% of cells sequenced to a depth of ≥5,000,000 total reads (median, ~8,700,000; range, ~3,800,000–84,300,000).

To identify cell types, we developed a classification approach that takes into account all expressed genes and is agnostic as to the origin of cells (Fig. 1*b*). Briefly, we applied two parallel and iterative approaches for dimensionality reduction and clustering, iterative principal component analysis (PCA), and iterative weighted gene coexpression network analysis (WGCNA); we then validated the cluster membership from each approach using a nondeterministic machine learning method (random forest). The results from these two parallel cluster identification approaches were intersected and subjected to another round of cluster membership validation. This step assessed the consistency of individual cell classification: we refer to the 1424 cells that were consistently classified into the same cluster as "core cells" and refer to the 255 cells that were classified into more than one cluster by the random forest approach as "intermediate cells" (Fig. 1*b*).

This analysis segregated cells into 49 distinct core clusters (Fig. 1*c*). On the basis of known markers for major cell classes, we identified 23 GABAergic neuronal clusters (*Snap25*$^+$, *Slc17a7*$^-$, *Gad1*$^+$); 19 glutamatergic neuronal clusters (*Snap25*$^+$, *Slc17a7*$^+$, *Gad1*$^-$); and 7 non-neuronal clusters (*Snap25*$^-$, *Slc17a7*$^-$, *Gad1*$^-$) (Fig. 1*c*).We assigned location and identity to cell types within VISp on the basis of three complementary lines of evidence: layer-enriching

NOTES

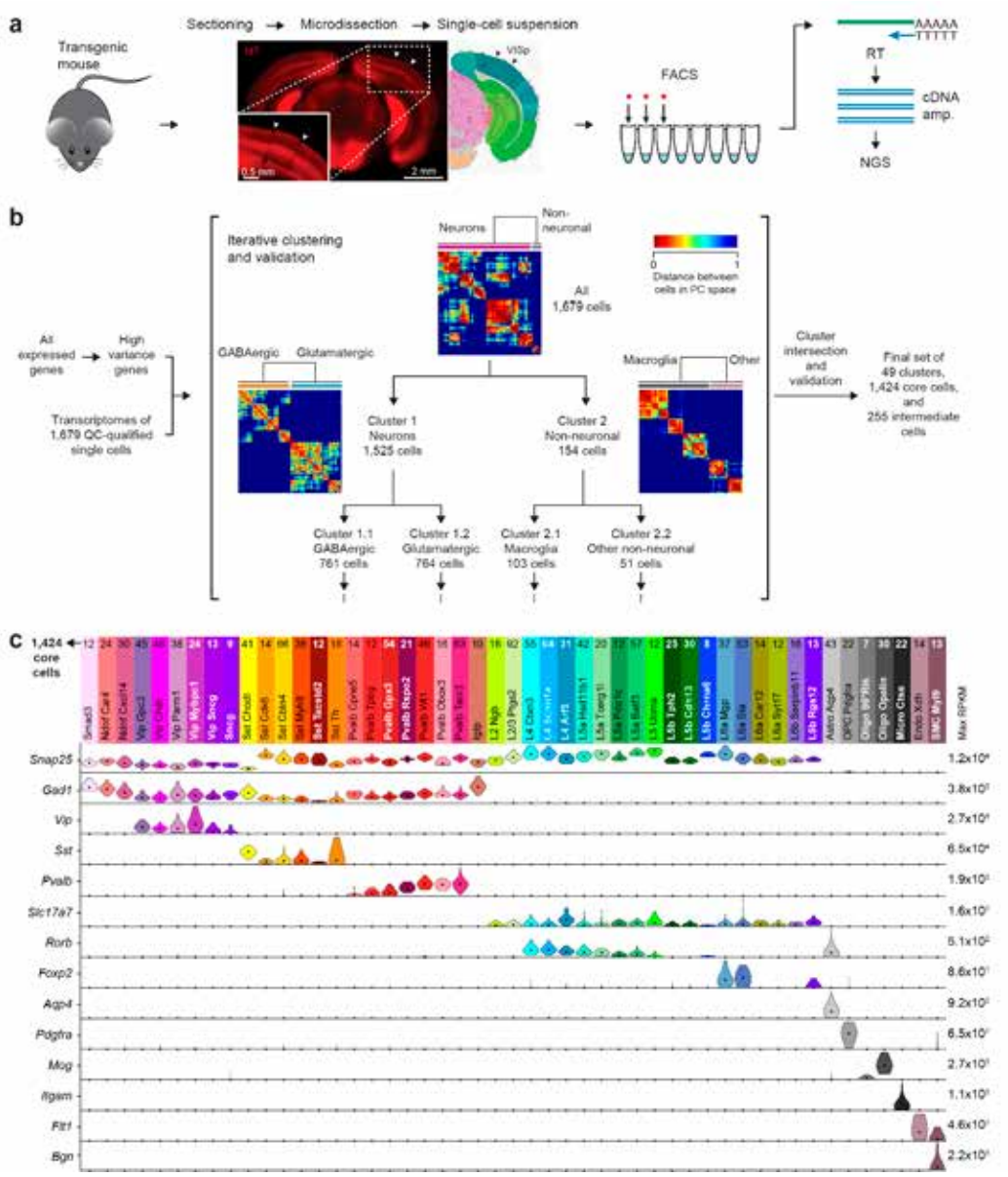

Figure 1. Workflow overview and cell-type identification. ***a,*** Experimental workflow started with the isolation, sectioning, and microdissection of the primary visual cortex from a transgenic mouse. The tissue samples were converted into a single-cell suspension; single cells were isolated by FACS; poly(A)-RNA from each cell was reverse transcribed (RT); and cDNA was amplified (SMARTer protocol, Clontech), tagmented (Nextera XT, Illumina), and sequenced on an NGS platform. ***b,*** Analysis workflow started with the definition of high-variance genes and iterative clustering based on two different methods—PCA (shown here) and WGCNA—and cluster membership validation using a random forest classifier. Cells that are classified consistently into one cluster are referred to as "core cells" (N = 1424), whereas cells that are mapped to more than one cluster are labeled as "intermediate cells" (N = 255). After the termination criteria are met, clusters from the two methods are intersected and iteratively validated until all core clusters contain at least four cells. ***c,*** The final 49 clusters were assigned an identity based on cell location and marker gene expression. Each type is represented by a color bar with the name and number of core cells representing that type. The violin plots represent distribution of mRNA expression on a linear scale, adjusted for each gene (maximum RPKM on the right), for major known marker genes: *Snap25* (pan-neuronal); *Gad1* (pan-GABAergic); *Vip, Sst,* and *Pvalb* (GABAergic); *Slc17a7* (pan-glutamatergic); *Rorb* (mostly L4 and L5a); *Foxp2* (L6); *Aqp4* (astrocytes); *Pdgfra* (OPCs); *Mog* (oligodendrocytes); *Itgam* (microglia); *Flt1* (endothelial cells); and *Bgn* (SMCs). RPKM, reads per kilobase per million. Reprinted with permission from Tasic B et al. (2016), Adult mouse cortical cell taxonomy revealed by single cell transcriptomics, Nature Neuroscience 19:335–346, their Fig. 1. Copyright 2016, Nature Publishing Group.

NOTES

dissections from specific Cre lines, expression of previously reported and/or newly discovered marker genes in our RNA-seq data, and localized expression patterns of marker genes determined using RNA *in situ* hybridization (ISH) (Tasic et al., 2016).

Our single-cell analysis detects most previously known marker genes and identifies many new differentially expressed genes. For a select set of markers, we used single-label and double-label RNA ISH and quantitative reverse transcription PCR (qRT-PCR) to confirm predicted specificity of marker expression or cell location obtained from layer-enriching dissections (Tasic et al., 2016). Our Cre line–based approach also enabled the characterization of these lines' specificity, thereby informing their proper use for labeling and perturbing specific cellular populations (Taniguchi et al., 2011; Olsen et al., 2012; Harris et al., 2014; Huang, 2014). In general, we found that the examined Cre lines mostly label the expected cell types based on promoters and other genetic elements that control Cre recombinase expression in each line; however, all but one Cre line (*Chat-IRES-Cre*) labeled more than one transcriptomic cell type (Tasic et al., 2016).

Cortical Cell Types: Markers and Relationships

To provide an overall view of the transcriptomic cell types that we identified, we integrated our data into constellation diagrams that summarize the identity, select marker genes, and putative location of these types along the pia-to-white-matter axis (Figs. 2*a*–*c*). In these diagrams, each transcriptomic cell type is represented by a disk whose surface area corresponds to the number of core cells in our dataset belonging to that type. Intermediate cells are represented by lines connecting the disks; the line thickness is proportional to the number of intermediate cells. We separately present GABAergic, glutamatergic, and non-neuronal constellations because we detected only a single intermediate cell between these major classes. This mode of presentation paints the overall phenotypic landscape of cortical cell types as a combination of continuity and discreteness: the presence of a large number of intermediate cells between a particular pair of core types suggests a phenotypic continuum, whereas a lack of intermediate cells connecting one type to others suggests its more discrete character (Figs. 2*a*–*c*). We represent the overall similarity of gene expression between the transcriptomic cell types by hierarchical clustering of groups of their core cells based on all genes expressed above a variance threshold (Fig. 2*d*). These two views of transcriptomic cell types are complementary: one shows the extent of intermediate phenotypes, and the other shows the overall similarity in gene expression among cluster cores.

We identified 18 transcriptomic cell types belonging to three previously described major classes of GABAergic cells named after the corresponding markers Vip (vasoactive intestinal peptide), Pvalb (parvalbumin), and Sst (somatostatin) (Gonchar et al., 2008; Xu et al., 2010; Rudy et al., 2011). In a substantial portion of these cells, we detected more than one of these markers; however, our method, which takes into account genome-wide gene expression, usually classified these double-expressing cells into the major type corresponding to the most highly expressed major marker in that cell.

We identified five additional GABAergic types. In accord with a previous report (Pfeffer et al., 2013), we detected *Tnfaip8l3* and *Sema3c* in these types. We named two of them on the basis of a gene for a putative neuropeptide—neuron-derived neurotrophic factor (*Ndnf*)—and we found that they corresponded to neurogliaform cells (Tasic et al., 2016). We refer to the three other types according to markers they express: synuclein gamma (*Sncg*), interferon gamma–induced GTPase (*Igtp*), and SMAD family member 3 (*Smad3*).

Beyond the major types, correspondence of our transcriptomic types to those previously described in the literature was not straightforward and relied on the existence of a Rosetta stone: a shared reagent, feature, or molecular marker with unambiguous translational power. Potential inferences on correspondence to previously proposed types were further complicated by previous studies' use of a variety of animal models, at various ages, focusing on different cortical areas and a few molecular markers (Rudy et al., 2011; DeFelipe et al., 2013).

We found only one Sst type (Sst-Cbln4) that was prevalent in upper cortical layers, whereas all the other Sst types appeared to be enriched in lower layers (Fig. 2*a*) (Tasic et al., 2016). On the basis of upper-layer enrichment and *Calb2* expression of the Sst-Cbln4 type, we propose that it likely corresponds to previously characterized Calb2-positive Martinotti cells that are enriched in the upper cortical layers (Xu et al., 2006) and are fluorescently labeled in transgenic *GIN* (GABAergic interneuron) mice (Oliva et al., 2000). Our analysis revealed only one additional *Calb2*-positive Sst type, which we refer to as Sst-Chodl. On the basis of the expression of tachykinin-receptor 1 (*Tacr1*), neuropeptide Y

NOTES

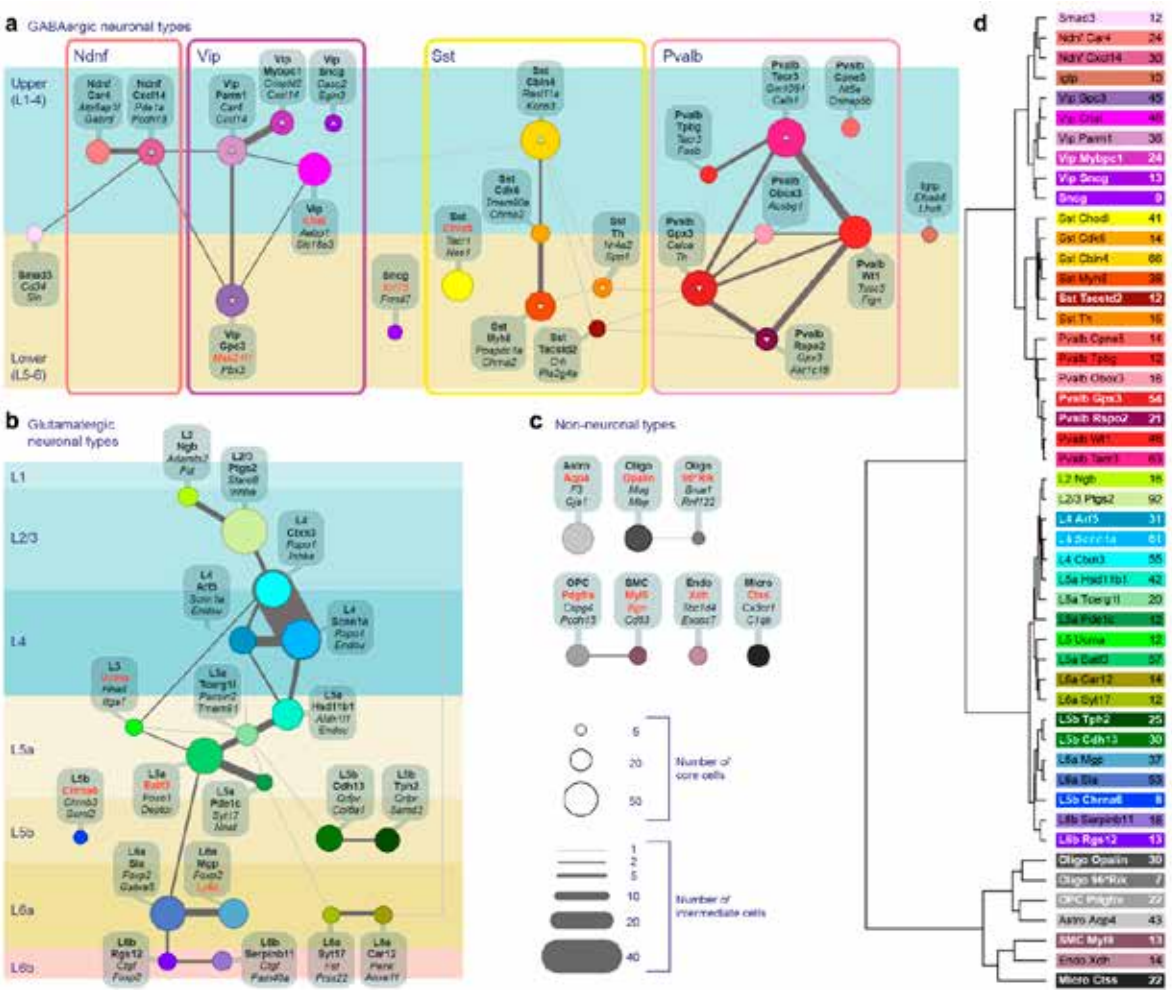

Figure 2. Cell-type summary and relationships. ***a–c,*** Constellation diagrams showing core and intermediate cells for all cell types. Core cells (*N* = 1424; 664 GABAergic, 609 glutamatergic, and 151 non-neuronal) are represented by colored disks with areas corresponding to the number of core cells for each cluster. Linked tags include cell-type names based on marker genes and layers; unique markers are in red. Intermediate cells (*N* = 255; 97 GABAergic, 155 glutamatergic, and 3 non-neuronal) are represented by lines connecting disks; line thickness corresponds to the number of such cells. ***a,*** GABAergic types are grouped according to major classes and arranged by their preferential location (enrichment) in upper versus lower cortical layers. Up and down arrows in disks represent statistically significant enrichment determined by layer-enriching dissections. Locations for other clusters are estimates that combine marker gene expression or Cre-line expression based on RNA ISH. The position at the border of upper and lower layers represents lack of evidence for location preference. ***b,*** Glutamatergic types are arranged according to cortical layer. ***c,*** Non-neuronal types share few intermediate cells with one another. *96*Rik, 9630013A20Rik*. ***d,*** Dendrogram depicting relatedness of the mean gene expression pattern for all cell types based on core cells (*N* = 1424) and genes (*N* = 13,878) with SD for expression >1 across all types. The distance metric is Pearson's correlation coefficient over the genes in the $\log_{10}$(RPKM+1) space. The tree was generated using standard hierarchical clustering with average linkage. RPKM, reads per kilobase per million. Reprinted with permission from Tasic B et al. (2016), Adult mouse cortical cell taxonomy revealed by single cell transcriptomics, Nature Neuroscience 19:335–346, their Fig. 4. Copyright 2016, Nature Publishing Group.

NOTES

(*Npy*), high levels of nitric oxide synthase (*Nos1*), and the absence of *Calb1* (Tasic et al., 2016), we concluded that this type most likely corresponds to Nos1 type I neurons (Seress et al., 2005). Nos1 type I neurons are enriched in L5 and 6 (Lee and Jeon, 2005) and are likely long-range projecting (Tomioka et al., 2005), sleep-active neurons (Gerashchenko et al., 2008).

The Pvalb types are highly interconnected in the constellation diagrams (Fig. 2*a*). Using layer-enriching dissections, we found that some types were preferentially present in upper (Pvalb-Tpbg, Pvalb-Tacr3, Pvalb-Cpne5) or lower (Pvalb-Gpx3 and Pvalb-Rspo2) layers (Tasic et al., 2016). To relate our transcriptomic types to previously described Pvalb types, we isolated cells from the upper layers of the *Nkx2.1-CreERT2* line, which, when induced with tamoxifen perinatally, labels a subset of neocortical interneurons, including chandelier cells (Taniguchi et al., 2013). Our analysis classified cells from this line in all three upper layer–enriched Pvalb types (Tasic et al., 2016). We suggest that Pvalb-Cpne5 corresponds to chandelier cells for several reasons: it was most transcriptionally distinct among Pvalb types, it was enriched in upper layers, and it did not express *Etv1* (also known as *Er81*), as previously shown for chandelier cells (Dehorter et al., 2015).

The Vip major class can be divided into several transcriptomic cell types, all of which appeared to be enriched in upper cortical layers, except the Vip-Gpc3 type (Fig. 2*a*). In accord with previous reports (von Engelhardt et al., 2007; Gonchar et al., 2008), our Vip-Chat transcriptomic type was located in upper cortical layers and displayed unique expression of choline acetyltransferase (*Chat*) in Vip-positive cells. These cells have been reported to either express (von Engelhardt et al., 2007) or not express Calb2 at the protein level (Gonchar et al., 2008); we found that they robustly expressed *Calb2* mRNA.

For glutamatergic cells, we identified six major classes of transcriptomic types—L2/3, L4, L5a, L5b, L6a, and L6b—on the basis of the layer-specific expression of marker genes and layer-enriching dissections (Fig. 2*b*); this is consistent with many previous studies (Lein et al., 2007; Molyneaux et al., 2007; Greig et al., 2013; Sorensen et al., 2013). We discovered subdivisions among all of these layer-specific major types. In L2/3, we identified two major types, one of which (L2-Ngb) appeared to be located more superficially based on marker gene expression (for example, *Ngb*, *Fst*, *Syt17*, and *Cdh13*). In L4, we identified three types (L4-Ctxn3, L4-Scnn1a, and L4-Arf5) with high gene expression similarity (Fig. 2*d*) and a large number of intermediate cells (Fig. 2*b*). We identified eight different transcriptomic types in L5. Four of these types expressed the L5a marker *Deptor* (L5a-Hsd11b1, L5a-Tcerg1l, L5a-Batf3, and L5a-Pde1c), whereas three expressed the L5b marker *Bcl6* (L5b-Cdh13, L5b-Tph2, and L5b-Chrna6). One of these L5b types (L5b-Chrna6), together with the L5-Ucma type, appeared most distinct among L5 types, on the basis of both gene expression and the small number of intermediate cells between them and other L5 types (Fig. 2*b*). We identified six transcriptomic cell types in L6: four L6a types and two L6b types. Among L6a types, two highly related types (L6a-Sla and L6a-Mgp) expressed the marker *Foxp2* (Molyneaux et al., 2007; Zeng et al., 2012; Sorensen et al., 2013) and were derived primarily from the *Ntsr1-Cre* line, whereas the other two (L6a-Syt17 and L6a-Car12) did not express *Foxp2* and were isolated as tdT^- cells from L6 of the same Cre line. For the latter two types, we discovered several new markers that can be used to identify them (*Car12*, *Prss22*, *Syt17*, and *Penk*). The two L6b types (L6b-Serpinb11 and L6b-Rgs12) expressed the known L6b marker *Ctgf* (Molyneaux et al., 2007; Zeng et al., 2012; Sorensen et al., 2013) and several other previously identified L6b markers (e.g., *Trh*, *Tnmd*, and *Mup5*) (Sorensen et al., 2013).

Despite the neuronal focus of this study, our sampling strategy captured enough cells to identify the major non-neuronal classes. We found seven non-neuronal types: astrocytes, microglia, oligodendrocyte precursor cells (OPCs), two types of oligodendrocytes, endothelial cells, and smooth muscle cells (SMCs). In accord with previous population-level studies (Cahoy et al., 2008; Zhang et al., 2014), these types could be distinguished by many combinatorial and unique markers (Figs. 1*c* and 2*c*).

Discussion and Outlook

The adult mouse visual cortex contains ~1,000,000 cells, of which approximately half are neurons (Herculano-Houzel et al., 2013) that can be divided into glutamatergic (80%) and GABAergic cells (20%) (DeFelipe, 2002). Our description of the 49 transcriptomic cortical cell types includes all the major types reported in the literature, some additional new types, as well as subdivisions among the major types. Our approach also provides an experimental and computational workflow to systematically catalog cell types in any region of the mouse brain and relate them to the tools used to examine those cell types (Cre lines and viruses). The discovery of new marker genes enables the generation of new specific Cre lines

NOTES

and provides guidance for intersectional transgenic strategies (Tasic et al., 2016) to enable specific access to cortical cell types that do not express unique marker genes.

Our method relies on dissociation and FACS isolation of single cells, thereby exposing them to stress that might lead to changes in gene expression. However, in our dataset, the majority of marker genes showed excellent correspondence to RNA ISH data from the Allen Brain Atlas (Lein et al., 2007) (~72% of 228 examined genes), suggesting that our procedure did not markedly alter the transcriptional signatures of cell types. Most of the other examined transcripts in this set, which appeared to be very specific markers based on RNA-seq and qRT-PCR (for example, *Chodl*), were not detected by the Allen Brain Atlas in VISp. This discrepancy is probably a consequence of low sensitivity for a subset of ISH probes.

To classify cells based on their transcriptomes, we used two iterative clustering methods and one machine learning–based validation method. The latter assessed the robustness of cluster membership for each cell and suggested the existence of cells with intermediate transcriptomic phenotypes. Previous studies either excluded intermediate cells explicitly (Macosko et al., 2015) or allowed cells to have only a single identity (Usoskin et al., 2014; Pollen et al., 2015; Zeisel et al., 2015). We chose to develop a data analysis approach that accommodates these intermediate cells, as they may be a reflection of actual phenotypic continua. However, as in any approach, both biological and technical aspects contributed to our datasets. For example, similarly to a previous single-cell transcriptomic study (Zeisel et al., 2015), we estimate that we detected only ~23% of mRNA molecules present in a cell (Tasic et al., 2016). Use of a highly efficient transcriptomic method that sampled the cells in their native environment and in proportion to their abundance would provide a more complete and accurate description of the transcriptomic cell-type landscapes. Inclusion of additional cells, even with the current method, is likely to segregate some of the types we defined here into additional subtypes. This subdivision is already apparent in our dataset, as we observed more subtypes if we decreased the threshold for the minimal number of core cells required to define a type (Tasic et al., 2016). In contrast, additional cell sampling may also reveal previously undetected intermediate cells that would define new continua between discrete types. Finally, although we attempted to cover all major types by choosing a variety of Cre lines, including pan-glutamatergic and pan-GABAergic lines, it is still possible we did not sample some rare types.

We used substantially deeper sequencing per cell than several other studies did (Jaitin et al., 2014; Pollen et al., 2014; Macosko et al., 2015). One of the main advantages of low-depth sequencing is reduction of experimental cost. However, we note that when we downsampled our data from full depth to 1,000,000 or 100,000 mapped reads per cell, we lost the power to detect many types (Tasic et al., 2016). Thus, when subsampling to 100,000 reads, we found only 35 types instead of 49. This decrease in resolution could be compensated for by sampling many more cells, but the appropriate balance between sequencing depth and cell number depends on a variety of factors, including the selected RNA-seq method, informative transcript abundance, tissue and cell-type abundance/accessibility, and desired resolution between cell types.

Our results suggest many new directions for further investigation. At the forefront is the question of the correspondence and potential causal relationships between transcriptomic signatures and specific morphological, physiological, and functional properties. Are certain transcriptomic differences representative of cell state or activity, rather than cell type? In fact, is there a clear distinction between the state and the type? For example, recent evidence suggests that Pvalb basket cells acquire specific firing properties in an activity-dependent manner that may result in a continuum of basket-cell phenotypes (Dehorter et al., 2015), perhaps mirroring the large numbers of intermediate cells that we found for upper-layer *Etv1*(*Er81*)–positive Pvalb cells (Fig. 2a). Although these questions await further studies, our approach provides an overview of adult cell types in a well-defined cortical area based on a highly multidimensional dataset and is an essential step toward understanding the most complex animal organ—the mammalian brain.

Acknowledgments

This paper was excerpted with permission, with minor modifications, from Tasic B et al. (2016) Adult mouse cortical cell taxonomy revealed by single cell transcriptomics, *Nature Neuroscience* 19:335–346, copyright 2016, Nature Publishing Group. The author would like to thank the Allen Institute for Brain Science founders, Paul G. Allen and Jody Allen, for their vision, encouragement, and support.

References

Belgard TG, Marques AC, Oliver PL, Abaan HO, Sirey TM, Hoerder-Suabedissen A, Garcia-Moreno F, Molnar Z, Margulies EH, Ponting CP (2011) A transcriptomic atlas of mouse neocortical layers. Neuron 71:605–616.

Cahoy JD, Emery B, Kaushal A, Foo LC, Zamanian JL, Christopherson KS, Xing Y, Lubischer JL, Krieg PA, Krupenko SA, Thompson WJ, Barres B (2008). A transcriptome database for astrocytes, neurons, and oligodendrocytes: a new resource for understanding brain development and function. J Neurosci 28:264–278.

DeFelipe J (2002) Cortical interneurons: from Cajal to 2001. Prog Brain Res 136:215–238.

DeFelipe J, López-Cruz PL, Benavides-Piccione R, Bielza C, Larrañaga P, Anderson S, Burkhalter A, Cauli B, Fairén A, Feldmeyer D, Fishell G, Fitzpatrick D, Freund TF, González-Burgos G, Hestrin S, Hill S, Hof PR, Huang J, Jones EG, Kawaguchi Y, et al. (2013). New insights into the classification and nomenclature of cortical GABAergic interneurons. Nat Rev Neurosci 14:202–216.

Dehorter N, Ciceri G, Bartolini G, Lim L, del Pino I, Marin O (2015) Tuning of fast-spiking interneuron properties by an activity-dependent transcriptional switch. Science 349:1216–1220.

Doyle JP, Dougherty JD, Heiman M, Schmidt EF, Stevens TR, Ma G, Bupp S, Shrestha P, Shah RD, Doughty ML, Gong S, Greengard P, Heintz N (2008). Application of a translational profiling approach for the comparative analysis of CNS cell types. Cell 135:749–762.

Gerashchenko D, Wisor JP, Burns D, Reh RK, Shiromani PJ, Sakurai T, de la Iglesia HO, Kilduff TS (2008) Identification of a population of sleep-active cerebral cortex neurons. Proc Natl Acad Sci USA 105:10227–10232.

Glickfeld LL, Reid RC, Andermann ML (2014) A mouse model of higher visual cortical function. Curr Opin Neurobiol 24:28–33.

Gonchar Y, Wang Q, Burkhalter AH (2008) Multiple distinct subtypes of GABAergic neurons in mouse visual cortex identified by triple immunostaining. Front Neuroanat 1:3.

Greig LC, Woodworth MB, Galazo MJ, Padmanabhan H, Macklis JD (2013) Molecular logic of neocortical projection neuron specification, development and diversity. Nat Rev Neurosci 14:755–769.

Harris JA, Hirokawa KE, Sorensen SA, Gu H, Mills M, Ng LL, Bohn P, Mortrud M, Ouellette B, Kidney J, Smith KA, Dang C, Sunkin S, Bernard A, Oh SW, Madisen L, Zeng H (2014). Anatomical characterization of Cre driver mice for neural circuit mapping and manipulation. Front Neural Circuits 8:76.

Harris KD, Shepherd GM (2015) The neocortical circuit: themes and variations. Nat Neurosci 18:170–181.

Hawrylycz MJ, Lein ES, Guillozet-Bongaarts AL, Shen EH, Ng L, Miller JA, van de Lagemaat LN, Smith KA, Ebbert A, Riley ZL, Abajian C, Beckmann CF, Bernard A, Bertagnolli D, Boe AF, Cartagena PM, Chakravarty MM, Chapin M, Chong J, Dalley RA, et al. (2012). An anatomically comprehensive atlas of the adult human brain transcriptome. Nature 489:391–399.

Hempel CM, Sugino K, Nelson SB (2007) A manual method for the purification of fluorescently labeled neurons from the mammalian brain. Nat Protoc 2:2924–2929.

Herculano-Houzel S, Watson C, Paxinos G (2013) Distribution of neurons in functional areas of the mouse cerebral cortex reveals quantitatively different cortical zones. Front Neuroanat 7:35.

Huang ZJ (2014) Toward a genetic dissection of cortical circuits in the mouse. Neuron 83:1284–1302.

Jaitin DA, Kenigsberg E, Keren-Shaul H, Elefant N, Paul F, Zaretsky I, Mildner A, Cohen N, Jung S, Tanay A, Amit I (2014) Massively parallel single-cell RNA-seq for marker-free decomposition of tissues into cell types. Science 343:776–779.

Lee JE, Jeon CJ (2005) Immunocytochemical localization of nitric oxide synthase-containing neurons in mouse and rabbit visual cortex and co-localization with calcium-binding proteins. Mol Cells 19:408–417.

Lein ES, Hawrylycz MJ, Ao N, Ayres M, Bensinger A, Bernard A, Boe AF, Boguski MS, Brockway KS, Byrnes EJ, Chen L, Chen L, Chen TM, Chin MC, Chong J, Crook BE, Czaplinska A, Dang CN, Datta S, Dee NR, et al. (2007) Genome-wide atlas of gene expression in the adult mouse brain. Nature 445:168–176.

NOTES

NOTES

Macosko EZ, Basu A, Satija R, Nemesh J, Shekhar K, Goldman M, Tirosh I, Bialas AR, Kamitaki N, Martersteck EM, Trombetta JJ, Weitz DA, Sanes JR, Shalek AK, Regev A, McCarroll SA (2015) Highly parallel genome-wide expression profiling of individual cells using nanoliter droplets. Cell 161:1202–1214.

Molyneaux BJ, Arlotta P, Menezes JR, Macklis JD (2007) Neuronal subtype specification in the cerebral cortex. Nat Rev Neurosci 8:427–437.

Oliva AA Jr, Jiang M, Lam T, Smith KL, Swann JW (2000) Novel hippocampal interneuronal subtypes identified using transgenic mice that express green fluorescent protein in GABAergic interneurons. J Neurosci 20:3354–3368.

Olsen SR, Bortone DS, Adesnik H, Scanziani M (2012) Gain control by layer six in cortical circuits of vision. Nature 483:47–52.

Pfeffer CK, Xue M, He M, Huang ZJ, Scanziani M (2013) Inhibition of inhibition in visual cortex: the logic of connections between molecularly distinct interneurons. Nat Neurosci 16:1068–1076.

Pollen AA, Nowakowski TJ, Shuga J, Wang X, Leyrat AA, Lui JH, Li N, Szpankowski L, Fowler B, Chen P, Ramalingam N, Sun G, Thu M, Norris M, Lebofsky R, Toppani D, Kemp DW 2nd, Wong M, Clerkson B, Jones BN, et al. (2014) Low-coverage single-cell mRNA sequencing reveals cellular heterogeneity and activated signaling pathways in developing cerebral cortex. Nat Biotechnol 32:1053–1058.

Pollen AA, Nowakowski TJ, Chen J, Retallack H, Sandoval-Espinosa C, Nicholas CR, Shuga J, Liu SJ, Oldham MC, Diaz A, Lim DA, Leyrat AA, West JA, Kriegstein AR (2015) Molecular identity of human outer radial glia during cortical development. Cell 163:55–67.

Rudy B, Fishell G, Lee S, Hjerling-Leffler J (2011) Three groups of interneurons account for nearly 100% of neocortical GABAergic neurons. Dev Neurobiol 71:45–61.

Seress L, Abraham H, Hajnal A, Lin H, Totterdell S (2005) NOS-positive local circuit neurons are exclusively axo-dendritic cells both in the neo- and archi-cortex of the rat brain. Brain Res 1056:183–190.

Sorensen SA, Bernard A, Menon V, Royall JJ, Glattfelder KJ, Desta T, Hirokawa K, Mortrud M, Miller JA, Zeng H, Hohmann JG, Jones AR, Lein ES (2013) Correlated gene expression and target specificity demonstrate excitatory projection neuron diversity. Cereb Cortex 25:433–449.

Sugino K, Hempel CM, Miller MN, Hattox AM, Shapiro P, Wu C, Huang ZJ, Nelson SB (2006) Molecular taxonomy of major neuronal classes in the adult mouse forebrain. Nat Neurosci 9:99–107.

Taniguchi H, He M, Wu P, Kim S, Paik R, Sugino K, Kvitsiani D, Fu Y, Lu J, Lin Y, Miyoshi G, Shima Y, Fishell G, Nelson SB, Huang ZJ (2011) A resource of Cre driver lines for genetic targeting of GABAergic neurons in cerebral cortex. Neuron 71:995–1013.

Taniguchi H, Lu J, Huang ZJ (2013) The spatial and temporal origin of chandelier cells in mouse neocortex. Science 339:70–74.

Tasic B, Menon V, Nguyen TN, Kim TK, Jarsky T, Yao Z, Levi B, Gray LT, Sorensen SA, Dolbeare T, Bertagnolli D, Goldy J, Shapovalova N, Parry S, Lee C, Smith K, Bernard A, Madisen L, Sunkin SM, Hawrylycz M, et al. (2016) Adult mouse cortical cell taxonomy revealed by single cell transcriptomics. Nat Neurosci 19:335–346.

Toledo-Rodriguez M, Blumenfeld B, Wu C, Luo J, Attali B, Goodman P, Markram H (2004) Correlation maps allow neuronal electrical properties to be predicted from single-cell gene expression profiles in rat neocortex. Cereb Cortex 14:1310–1327.

Tomioka R, Okamoto K, Furuta T, Fujiyama F, Iwasato T, Yanagawa Y, Obata K, Kaneko T, Tamamaki N (2005) Demonstration of long-range GABAergic connections distributed throughout the mouse neocortex. Eur J Neurosci 21:1587–1600.

Usoskin D, Furlan A, Islam S, Abdo H, Lonnerberg P, Lou D, Hjerling-Leffler J, Haeggstrom J, Kharchenko O, Kharchenko PV, Linnarsson S, Ernfors P (2014) Unbiased classification of sensory neuron types by large-scale single-cell RNA sequencing. Nat Neurosci 18:145–153.

von Engelhardt J, Eliava M, Meyer AH, Rozov A, Monyer H (2007) Functional characterization of intrinsic cholinergic interneurons in the cortex. J Neurosci 27:5633–5642.

Xu X, Roby KD, Callaway EM (2006) Mouse cortical inhibitory neuron type that coexpresses somatostatin and calretinin. J Comp Neurol 499:144–160.

Xu X, Roby KD, Callaway EM (2010) Immunochemical characterization of inhibitory mouse cortical neurons: three chemically distinct classes of inhibitory cells. J Comp Neurol 518:389–404.

Zeisel A, Muñoz-Manchado AB, Codeluppi S, Lonnerberg P, La Manno G, Juréus A, Marques S, Munguba H, He L, Betsholtz C, Rolny C, Castelo-Branco G, Hjerling-Leffler J, Linnarsson S (2015) Brain structure. Cell types in the mouse cortex and hippocampus revealed by single-cell RNA-seq. Science 347:1138–1142.

Zeng H, Shen EH, Hohmann JG, Oh SW, Bernard A, Royall JJ, Glattfelder KJ, Sunkin SM, Morris JA, Guillozet-Bongaarts AL, Smith KA, Ebbert AJ, Swanson B, Kuan L, Page DT, Overly CC, Lein ES, Hawrylycz MJ, Hof PR, Hyde TM, et al. (2012) Large-scale cellular-resolution gene profiling in human neocortex reveals species-specific molecular signatures. Cell 149:483–496.

Zhang C, Frias MA, Mele A, Ruggiu M, Eom T, Marney CB, Wang H, Licatalosi DD, Fak JJ, Darnell RB (2010) Integrative modeling defines the Nova splicing-regulatory network and its combinatorial controls. Science 329:439–443.

Zhang Y, Chen K, Sloan SA, Bennett ML, Scholze AR, O'Keeffe S, Phatnani HP, Guarnieri P, Caneda C, Ruderisch N, Deng S, Liddelow SA, Zhang C, Daneman R, Maniatis T, Barres BA, Wu JQ (2014) An RNA-sequencing transcriptome and splicing database of glia, neurons, and vascular cells of the cerebral cortex. J Neurosci 34:11929–11947.

NOTES